

NON-LTE INVERSION OF LINE PROFILES

H. SOCAS-NAVARRO, B. RUIZ COBO, AND J. TRUJILLO BUENO

Instituto de Astrofísica de Canarias, E-38200, La Laguna (Tenerife), Spain

Received 1998 April 15; accepted 1998 June 10

ABSTRACT

In this paper we address the problem of the non-LTE (NLTE) inversion of line profiles by means of a nonlinear least-squares minimization procedure combined with very efficient multilevel transfer methods. Our approach is based on the concept of response functions, which measure the first-order response of the emergent profiles to changes in the atmospheric conditions. We introduce the fixed departure coefficients (FDC) approximation in order to compute these response functions in a fast and straightforward manner. The accuracy of this approximation is checked comparing FDC response functions with those obtained from full NLTE computations. An NLTE inversion code based on these response functions has been developed and extensively tested. Reference synthetic profiles, similar to those expected from real observations, are given as input to the inversion algorithm and the recovered models are shown to be compatible with the reference models within the error bars. Our NLTE inversion code thus provides a new tool for the investigation of the chromospheres of the Sun and other stars.

Subject headings: line: profiles — radiative transfer — stars: chromospheres — Sun: chromosphere

1. INTRODUCTION

Inversion codes have been extensively used since the early 1970s to seek for model atmospheres that produce synthetic profiles more or less similar to the observations presented as input. Although important efforts have been carried out, it is clear that the currently applied diagnostic tools are not yet able to account for all the (known) relevant physical processes involved in the radiative transfer, and therefore valuable information contained in the observations is being thrown away. Since the technological development is allowing for the design of increasingly accurate instrumentation, the need for new, more sophisticated, analysis techniques becomes more obvious every day.

Among the problems that have not yet been tackled properly, we consider of paramount importance the semi-empirical modeling of stellar chromospheres, which is the main focus of our work. It is our belief that the development of an inversion code suitable for application to line profiles for which the approximation of local thermodynamic equilibrium (LTE) is not appropriate will become a very valuable diagnostic tool to obtain further insights into this region of the atmosphere that still remains poorly understood.

Two noteworthy works have been carried out aiming at the recovery of information from the spectral profiles of strong non-LTE (NLTE) lines. Mein et al. (1987) developed a procedure based on the Fourier analysis of the spectrum. They synthesized reference profiles from a solar model atmosphere and related the deviations of the observations from these synthetic profiles to departures of the real Sun from their reference atmosphere. However, only four free parameters are recovered in this manner. These are some “mean” values of the velocity, velocity gradient, temperature, and temperature gradient. They applied their method to the study of the Ca II H and K resonance lines under the assumption of complete angle and frequency redistribution and neglecting or prescribing microturbulence and macroturbulence.

Another inversion effort was carried out by Teplitskaya, Skochilov, & Grigoryeva (1992) and Teplitskaya, Turova, & Skochilov (1992) who applied the Tikhonov regulariza-

tion method to solve the radiative transfer equation as a Fredholm equation of the first kind for the source function. They assumed that the total source function can be approximated by the line source function, which is a valid approximation near the core of strong lines only. In these papers, complete redistribution was assumed. More recently Teplitskaya, Grigoryeva, & Skochilov (1996) have shown that their technique can be generalized to partial redistribution. Although they succeed in recovering the line source function, they did not show how to recover any atmospheric information from this inversion.

In this paper, we extend to NLTE the inversion approach of Ruiz Cobo & del Toro Iniesta (1992). They presented a method, based on the concept of response functions, for the inversion of Stokes profiles of spectral lines under the assumption of LTE and one-dimensional plane-parallel atmosphere. The LTE inversion code, known as SIR (Stokes Inversion based on Response functions) allows for the recovery of the depth-dependent temperature, pressure, microturbulence, line-of-sight velocity, and magnetic field vector, as well as some unevaluated parameters, like macroturbulence or percentage of stray light.

Several works have been carried out with the strategy described in that paper. Successful applications include the study of sunspots (Collados et al. 1994; del Toro Iniesta, Tarbell, & Ruiz Cobo 1994; Westendorp Plaza et al. 1997a, 1997b), thin flux tubes (Bellot Rubio, Ruiz Cobo, & Collados 1997), the solar granulation (Ruiz Cobo et al. 1995, 1996; Rodríguez Hidalgo, Ruiz Cobo, & Collados 1996), the photospheric 5 minute solar oscillations (Ruiz Cobo, Rodríguez Hidalgo, & Collados 1997), and the photospheres of cool stars (Allende Prieto, Ruiz Cobo, & García López 1998). Also, a different inversion code, but with a similar approach, has been developed by Sánchez Almeida (1997) for the study of microstructured magnetic atmospheres.

Up to now, these inversion techniques have always been applied under the LTE hypothesis, which has proven to be a reasonable approximation for a number of spectral lines synthesized with well-known solar models (Shchukina, Trujillo Bueno, & Kostik 1997; Shchukina & Trujillo Bueno

1997; Socas-Navarro et al. 1996). The LTE assumption has two major implications in the inversion procedure. First, the synthetic profile is very quickly computed, since the level populations for the atomic transition being considered are obtained from the solution of the Saha and Boltzmann equations, and the source function is given simply by the Planck function. The second, and more important, is that the response functions, which (as we will see below) are a key point for the success of the inversion algorithm, are easily calculated from the analytical derivatives of the level populations and the Planck function. The drawback is that LTE restricts the applicability range of the method to photospheric lines, and it cannot be used for the analysis of strong lines that give information on higher chromospheric layers.

Combining this inversion procedure, based upon the Marquardt method (see Marquardt 1963) and the SVD technique (see Press et al. 1986), with robust and efficient solution methods for the NLTE multilevel radiative transfer problem (see, e.g., Socas-Navarro & Trujillo Bueno 1997), we have developed an NLTE inversion code of spectral lines that is able to recover the thermodynamical variables through the solar atmosphere. We are currently working on the generalization of this code to deal with the full Stokes vector, in order to obtain information regarding the magnetic structure of the chromosphere. Our NLTE inversion code has been tested with simulated observations of noisy line profiles, and the results show that it is ready for its application to the inversion of real observations.

In § 2 we present an approximate method for the fast computation of NLTE response functions. As we will show these response functions constitute a key point of the inversion algorithm. The validity of this approximation is checked in § 3, comparing them with accurate NLTE response functions computed by means of a brute force numerical calculation (see below). Our NLTE inversion code is described in § 4, together with some tests that are shown in § 5. Finally, the main conclusions and the perspectives for the near future are outlined in § 6.

2. THE FIXED DEPARTURE COEFFICIENTS (FDC) APPROXIMATION

The response functions (hereafter RFs, see Mein 1971; Beckers & Milkey 1975; Caccin et al. 1977) measure the first-order reaction of the emergent intensity when a given model parameter is perturbed at a given depth. In our approach, the knowledge of this reaction is used by the inversion algorithm to calculate the first-order correction that should be applied to the various model parameters in order to compensate for the discrepancies between the synthetic and the observed profiles.

The most obvious way to evaluate RFs is to perturb each model parameter, synthesize a new “perturbed” profile, and take the ratio of the profile to the parameter perturbation. Such a “brute force” approach for the calculation of RFs can be regarded as very expensive in terms of CPU usage for most practical applications. Therefore, it is very important to have an alternative way of computing them. In LTE, analytical expressions exist for the derivatives involved, thus simplifying the problem of the calculation of the RFs. This is not the case in NLTE because of the lack of analytical expressions for the level population derivatives.

The FDC approximation is a straightforward generalization of the LTE derivatives, with NLTE populations

but assuming that the variations of the departure coefficients with the model parameters can be neglected. This FDC approximation greatly simplifies the problem, making the evaluation of the RFs as simple as in LTE.

In absence of magnetic fields and polarization phenomena, the radiative transfer equation can be written for each angle and frequency as (see, e.g., Mihalas 1978 for a derivation and the definition of the various symbols used)

$$\frac{d}{ds} I = \chi(S - I). \quad (1)$$

All the quantities that appear in equation (1) are angle and frequency dependent, but we will refrain from the use of any subscript to show this dependence, for notational simplicity.

Considering a small perturbation on the source function and the opacity in equation (1) and neglecting second-order and higher terms, we have that the reaction of the emergent intensity obeys a transfer equation that is formally identical to equation (1):

$$\frac{d}{ds} \delta I = \bar{\chi}(\delta S^{\text{eff}} - \delta I), \quad (2)$$

with

$$\delta S^{\text{eff}} = \delta S + \frac{\delta \chi}{\bar{\chi}} (\bar{S} - \bar{I}), \quad (3)$$

where \bar{f} is the unperturbed value and δf the perturbation. These perturbations on the source function and the opacity are, on their turn, caused by some original perturbation on the model atmosphere. If we discretize the atmosphere and denote by x the model parameter (i.e., the value of a quantity at a given depth, for instance the temperature at τ) that has been perturbed to yield δS and $\delta \chi$, it can be seen that the response of the emergent intensity to that particular parameter is

$$\frac{\partial I^{\text{syn}}}{\partial x} = R_x \Delta \tau = e^{-\tau} \left[\frac{\partial}{\partial x} S(\tau) \right] - \frac{1}{\chi(\tau)} \left[\frac{\partial}{\partial x} \chi(\tau) \right] (I - S)(\tau) \Delta \tau, \quad (4)$$

where R_x is the RF to x and $\Delta \tau$ is the grid spacing at τ . In the derivation of equation (4), it has been implicitly assumed that the derivatives of the opacity and the source function are local, i.e., that these quantities do not react to changes in the model parameters at other depth points. In general, this is not the case in NLTE but, as we will see below, the FDC approximation yields local derivatives for the opacity and the source function, and thus we can safely employ equation (4).

We first consider the opacity. If the line we are interested in is not blended, there are three contributors to the total opacity. These are the background continuum opacity (χ_c), the line opacity (χ_l), and the scattering term (σ). Thus, we can write down

$$\frac{\partial \chi}{\partial x} = \frac{\partial \chi_c}{\partial x} + \frac{\partial \sigma}{\partial x} + \frac{\partial \chi_l}{\partial x}. \quad (5)$$

Since χ_c and σ are computed from analytical expressions, their derivatives are known. The only quantity that depends upon the level populations is the line opacity:

$$\chi_l = \frac{h\nu}{4\pi} (n_l B_{lu} - n_u B_{ul}), \quad (6)$$

where B_{lu} and B_{ul} are the Einstein coefficients of the transition considered.

Computing NLTE populations and departure coefficients for the lower and upper levels of the transition (which we denote by b_l and b_u , respectively, where $b_i = n_i/n_i^*$) and using an asterisk to denote quantities that are evaluated in LTE, we find that the FDC approximation leads to

$$\frac{\partial \chi_l}{\partial x} \approx \frac{h\nu}{4\pi} \left(b_l \frac{\partial n_l^*}{\partial x} B_{lu} - b_u \frac{\partial n_u^*}{\partial x} B_{ul} \right). \quad (7)$$

We turn now to the derivatives of the source function. Again, since we have contributions that come from the background continuum, the line, and the scattering term, the total source function is given by

$$S = \frac{\chi_c}{\chi} S_c + \frac{\chi_l}{\chi} S_l + \frac{\sigma J}{\chi}, \quad (8)$$

where J is the mean intensity, defined as the angle average of the specific intensity. In LTE, the right-hand side of equation (8) reduces to the Planck function. Its derivatives are, then, straightforward. However, this is not the case in NLTE, where the derivatives of the line source function and the mean intensity are not known.

Consider first the line source function. For the sake of simplicity, the complete redistribution approximation (CRD) will be assumed throughout this paper. This hypothesis states that the line emission and absorption profiles have the same angle-frequency dependence and yields a line source function that is independent of the angle and frequency of the light beam considered. Thus, the line source function is given by

$$S_l = \frac{n_u A_{ul}}{n_l B_{lu} - n_u B_{ul}} = \frac{n_u^* A_{ul}}{(b_l/b_u) n_l^* B_{lu} - n_u^* B_{ul}}. \quad (9)$$

Then, with the FDC approximation, the sought derivatives can be expressed as

$$\frac{\partial S_l}{\partial x} \approx \frac{(\partial n_u^*/\partial x) A_{ul}}{(b_l/b_u) n_l^* B_{lu} - n_u^* B_{ul}} - \frac{n_u^* A_{ul} [(b_l/b_u) (\partial n_l^*/\partial x) B_{lu} - (\partial n_u^*/\partial x) B_{ul}]}{[(b_l/b_u) n_l^* B_{lu} - n_u^* B_{ul}]^2}. \quad (10)$$

The mean intensity J can be handled without any further assumptions. From its definition, it follows that

$$\frac{\partial J}{\partial x} = \frac{1}{4\pi} \int \frac{\partial I}{\partial x} d\Omega. \quad (11)$$

If we insert equation (4) in equation (11), calculate the derivatives of the line opacity and the line source function with the approximate expressions given by equation (7) and equation (10), and group all the known terms together, it turns out that

$$\frac{\partial J}{\partial x} = A + B \frac{\partial J}{\partial x}, \quad (12)$$

where A and B are known quantities. Solving this equation we find the derivatives of the mean intensity J :

$$\frac{\partial J}{\partial x} = \frac{A}{1 - B}. \quad (13)$$

However, we have not used equation (13) for the tests described in this paper. Instead, we have found that, in practice, it is enough to approximate the derivatives of the mean intensity by those of the Planck function. For the case of the strong NLTE lines that we are dealing with here, there is no need for an accurate treatment of this term. The wings of the line are formed in deeper layers of the atmosphere, where the source function is close to the Planck function. The core of the line, on its turn, is dominated by the line source function, and therefore the approximation chosen for the derivatives of J is of little relevance.

It is, then, straightforward to compute the derivatives of the source function and the opacity that enter in equation (4) to calculate approximate RFs. Thus, once we have the NLTE populations and departure coefficients for the model atmosphere given at each iterative step of the inversion procedure, the RFs are obtained without any additional computational expense as compared to the LTE case, and include information on NLTE effects through the departure coefficients.

3. FDC VERSUS STRICT RESPONSE FUNCTIONS

In order to check the validity of the FDC approximation for the RFs, we proceed now to compare these with “exact” RFs evaluated by means of a brute force approach. Each model parameter is perturbed at each depth point by a small amount, and the full NLTE problem is solved for this perturbed atmosphere in order to determine the sought response of the emergent profile. Figures 1 and 2 show the wavelength integrated RFs to the temperature for some Ca II and Mg I lines in two quiet Sun models and in a sunspot umbra model atmosphere. For the description of the quiet Sun atmosphere we have used the model C of Vernazza, Avrett, & Loesser (1981, hereafter referred to as VAL-C) and the model of Holweger & Müller (1974, hereafter referred to as HOLMUL), whereas for the sunspot umbra we chose the model M of Maltby et al. (1986, hereafter referred to as MACKKL).

In Figure 1 we depict RFs for the Ca II K line and the infrared triplet line at 8542 Å in the VAL-C model. We see that the FDC response presents a prominent peak in the highest atmospheric layers, whereas the true response is not that large. When we move to the HOLMUL model we find that the agreement is better. Note that only those atmospheric layers where the RFs are nonnegligible (i.e., where the lines are sensitive) can be accurately recovered by the inversion algorithm, as will be discussed below.

If we now consider in Figure 2 the Mg I lines, we find that in the VAL-C model the sensitivity to the chromospheric temperature is very small, and that the FDC approximation provides a good description. This lack of chromospheric sensitivity is important to understand the results of the inversion of these lines in § 5. Finally, we can see that in the MACKKL sunspot model, contrary to the VAL-C case, the Mg I lines are now sensitive to the chromospheric temperature and can be used for the thermodynamical diagnosis of this chromosphere.

We conclude that the FDC approximation fails to yield the right response in the highest regions of the atmosphere. However, in the framework of an inversion code, where the RFs are to be computed many times (one for each model estimation) and a brute force approach is not, in general, affordable in terms of CPU time, it becomes extremely valuable to count on such a fast technique for the computation

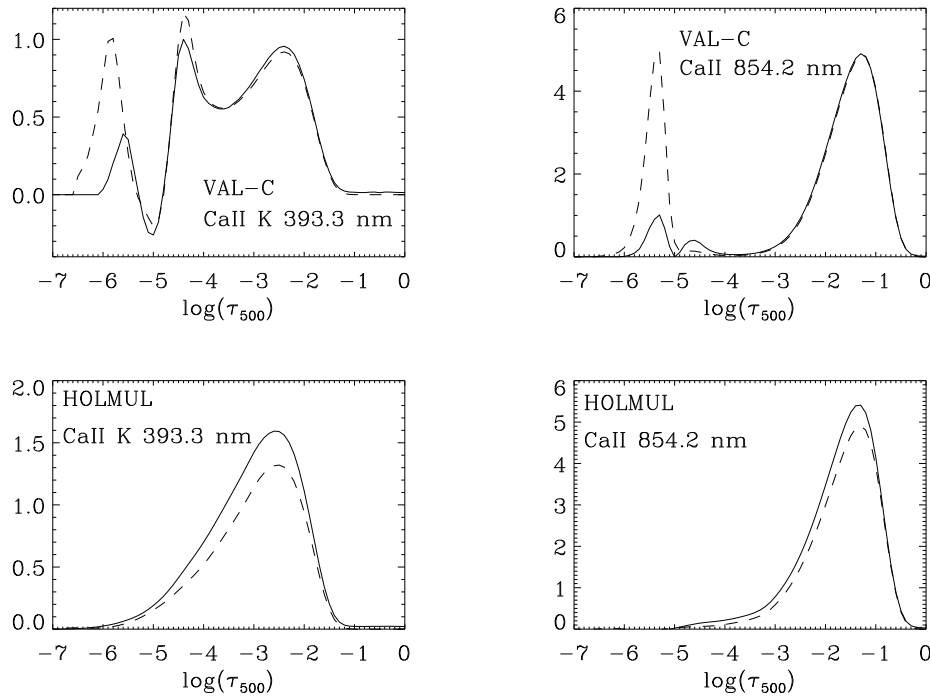


FIG. 1.—Wavelength integrated response functions to the temperature for two Ca II lines in the VAL-C and HOLMUL models, normalized to the maximum response of Ca II K line in the VAL-C model. *Solid line*: Full NLTE computation. *Dashed line*: FDC approximation.

of the RFs. In this manner, as we will show, we obtain a model by means of an FDC inversion that can be later used as the initialization for a further inversion step using accurate RFs.

4. DESCRIPTION OF THE CODE

Two nested iterative procedures are needed for the solution of the NLTE inversion problem with our approach. At the outer level we have the inversion iterations that modify

the model atmosphere to seek for the model that produces the best fit to the observed profiles. Then, at the inner level, the synthesis routine computes synthetic profiles emergent from the current model atmosphere considered by the inversion algorithm. This synthesis requires the evaluation of the atomic level populations that are consistent with the radiation field in the atmospheric model.

The problem of solving for NLTE level populations and line profiles has been deeply analyzed and, in absence of

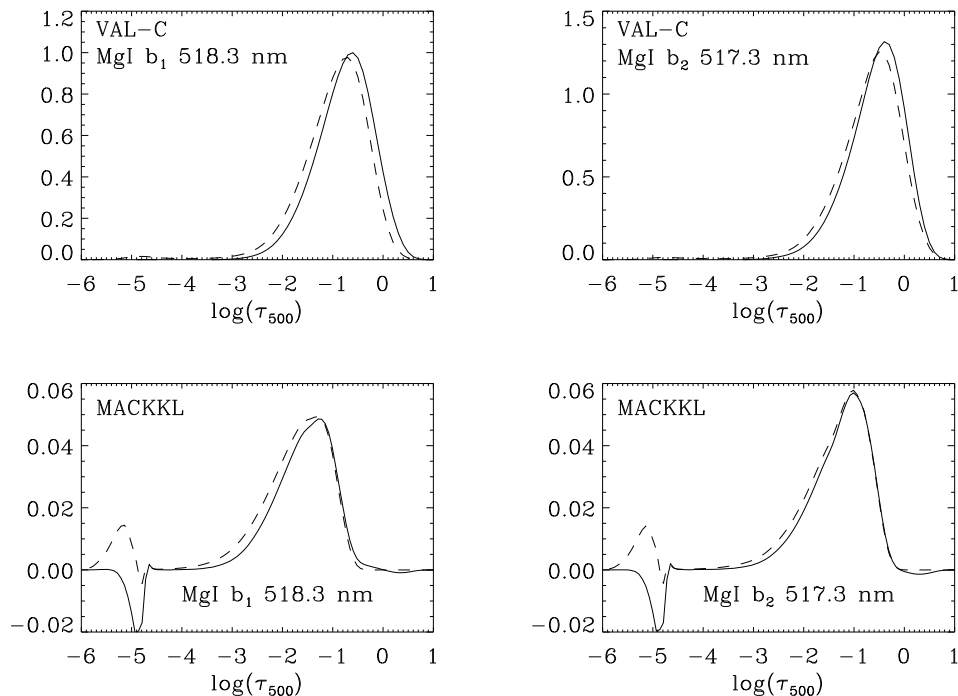


FIG. 2.—Wavelength integrated response functions to temperature of the Mg I b_1 and b_2 lines in the VAL-C and MACKKL models, normalized to the maximum response of Mg I b_1 in VAL-C. *Solid line*: Full NLTE computation. *Dashed line*: FDC approximation.

magnetic fields, reliable solutions have existed since the 1970s (see, e.g., Mihalas 1978; Kalkofen 1987). Dramatic improvements in efficiency have been achieved in the last few years (see Trujillo Bueno & Fabiani Bendicho 1995; Fabiani Bendicho, Trujillo Bueno, & Auer 1997), thus making possible the study of problems that were previously beyond the practical limits of computational possibilities. Three important categories of problems will greatly benefit from these new mathematical methods, namely, the multi-level transfer with very complex model atoms (> 100 levels), the application to multidimensional geometries, and problems where the radiative transfer must be solved many times. Our inversion technique lies precisely in this last category, as it iteratively modifies the current estimation of the model atmosphere, seeking for the best fitting model, and a new synthetic profile must be computed for each one of these intermediate atmospheres.

The main difficulties when facing the nonequilibrium problem arise for two reasons. The radiation field couples together all the populations through the whole atmosphere, and the atomic populations at a given depth are affected by perturbations of the medium at distant points. This is why the NLTE problem is said to be nonlocal. Moreover it is nonlinear. To emphasize this we write down the statistical equilibrium equations (also known as rate equations) that rule the population of the atomic levels:

$$\sum_{j \neq i} n_j (R_{ji} + C_{ji}) - n_i \sum_{j \neq i} (R_{ij} + C_{ij}) = 0. \quad (14)$$

In this equation C_{ij} and R_{ij} denote the collisional and radiative rates (transitions per unit volume and unit time) between levels i and j , respectively. The radiative rate R_{ij} depends on the frequency-averaged mean intensity \bar{J} , defined as

$$\bar{J} = \frac{1}{4\pi} \int d\Omega \int d\nu \phi_{\nu} I_{\nu}, \quad (15)$$

where I_{ν} is the specific intensity at a frequency ν that propagates along the ray direction Ω . This specific intensity depends upon the atomic level populations via the opacity and the source function in the radiative transfer equations. The nonlinearity and nonlocality is precisely due to this term, making necessary the development of iterative algorithms (see, e.g., Socas-Navarro & Trujillo Bueno 1997 for a critical discussion of this topic).

The NLTE part of our code employs a preconditioning-like scheme (see Rybicki & Hummer 1991, 1992) combined with a local, approximate Λ operator. This choice minimizes the memory storage and computing time per iteration, and it guarantees that positive populations are obtained at each iterative step. The level populations obtained in this manner are used to compute the emergent line profiles.

The inversion algorithm compares these synthetic emergent profiles with the observations and modifies the current atmosphere so that the new model produces synthetic profiles that fit better the observations, in a least-squares sense. The whole atmosphere is parameterized in terms of a set of free parameters called nodes (see Ruiz Cobo & del Toro Iniesta 1992), such that the corrections produced by the inversion algorithm in the nodes are interpolated by cubic splines to the rest of the atmosphere, which is then constructed from the old estimation and this interpolated correction. Therefore, we assume that the model sought does

not vary in a sharp manner between the nodes of the inversion, or to be more precise, that it can be reconstructed from smooth variations of the starting guess.

Some basic simplifying assumptions are introduced in the code both in the synthesis and in the inversion routines. For the synthesis, besides the CRD approximation mentioned above, we assume a one-dimensional plane-parallel atmosphere. The ionization equilibrium for the computation of the background opacities assumes that the ionization of the various metals occurs under LTE conditions. This approximation, which is often used by many authors, is very accurate for our purposes since we are mainly concerned with strong lines whose source function and opacity are dominated by line processes. The ionization equilibrium and background opacities are computed with standard opacity packages (see Kostik, Shchukina, & Rutten 1996).

The pressure through the atmosphere is given by the hydrostatic equilibrium equation, neglecting the terms coming from turbulent pressure and assuming that the upper boundary condition is known. A detailed treatment of the pressure stratification is above the scope of this paper, which deals only with the NLTE effects on the inversion, and it will be carefully addressed in a forthcoming paper, where the boundary condition for the integration of the hydrostatic equilibrium equation will be treated as another free parameter of the inversion.

For the error bars associated to the model parameter x_j , Sánchez Almeida (1997) derived the following formula:

$$\delta x_j^2 = \frac{1}{M} \chi^2 (\alpha^{-1})_{jj}, \quad (16)$$

where M is the number of free parameters, χ^2 is the merit function

$$\chi^2 = \sum_{i=1}^N \frac{(I_i^{\text{obs}} - I_i^{\text{syn}})^2}{\sigma_i^2}, \quad (17)$$

and α is the Hessian matrix

$$\alpha_{kl} = \frac{1}{2} \frac{\partial^2 \chi^2}{\partial x_k \partial x_l}. \quad (18)$$

We decided to adopt equation (16), but with a modification to consider the case where the misfitting is not uniformly distributed with the wavelength. To this aim we define a weighted χ_j^2 , which is different for each model parameter x_j , such that those wavelengths where x_j has a stronger influence (larger RFs) are taken into account with a larger weight:

$$\chi_j^2 = \frac{\sum_{i=1}^N R_{ij}^2 (I_i^{\text{obs}} - I_i^{\text{syn}})^2}{\sum_{i=1}^N \sigma_i^2 R_{ij}^2}. \quad (19)$$

In other words, the misfitting is *not* equally distributed among the various free parameters. This new definition reduces to equation (17) when (1) the wavelength dependence of the RFs to x_j is negligible (which means that x_j is equally responsible for the misfitting through the whole profile) or (2) the wavelength dependence of the misfitting is negligible.

This improvement is mandatory for our problem since, especially when a minimum of χ^2 has not yet been reached, the misfitting often varies strongly with the wavelength. The wings of the lines are then more accurately fitted than the core. In that case the recovered model is more reliable in the

photosphere than in the chromosphere, and this information must be accounted for by the error bars, which is what we aim with the definition of χ_f^2 given by equation (19).

5. INVERSION TESTS

For the examples in this section, we have chosen three different reference models to recover. With these models we synthesized several sets of spectral lines. After adding white noise to the lines in order to simulate real observations, they were presented to the inversion code. Three different models have been considered here: the quiet Sun VAL-C and HOLMUL models (hot and cool chromospheres, respectively), and the sunspot umbra MACKKL atmosphere.

A set of four strong chromospheric lines of Ca II plus a photospheric line of Fe I are synthesized with the VAL-C model and given as input to the inversion code. The Ca II lines chosen are the K line at 393.3 nm and the three lines of the infrared triplet at 849.4, 854.2, and 866.2 nm. The reference profiles of these lines are sampled with a resolution of 20 mÅ, covering a wavelength range of 2 Å for each line. The NLTE treatment is based on a five levels plus continuum model atom assuming complete redistribution (CRD) for all the transitions. Although this approximation has been shown to be accurate enough for the synthesis of the IR triplet, significant discrepancies are found in the core of the K line when partial redistribution effects are taken into account (see Uitenbroek 1989). However, for our testing purposes in this work, the validity of the CRD approximation is of little relevance, since both the synthetic and the (simulated) “observed” profiles have been calculated under CRD. Besides the chromospheric lines, the Fe I line at 6301 Å was included in the input data, in order to provide information on the photospheric layers of the model. It is treated in LTE, which is a reasonable approximation for this case (see Shchukina et al. 1997). White noise, simulating a signal-to-noise ratio in the continuum of 1000, was added to the reference profile.

As already mentioned, a full brute force treatment of the inversion problem requires large amounts of CPU time and it becomes prohibitive for some practical applications. However, if we are able to reach a model close enough to the solution using the FDC approximation, then the brute force approach dramatically reduces its computational requirements and becomes a perfectly feasible alternative. In the following tests, after initializing with very unrealistic isothermal models, we use our fast FDC-based inversion to recover a model that produces synthetic profiles more or less similar to the reference ones (see Figs. 3 and 4). Then, only numerical RFs to temperature are evaluated by perturbing the atmospheric variables at the nodes and solving the full NLTE problem to compute the “perturbed” synthetic profiles (i.e., in a brute force manner). The RF is, in fact, the ratio of the profile perturbation to the model parameter perturbation. We assume that our model is already close to the final solution, and thus the response will not vary significantly between iterations. Therefore, these RFs are kept fixed and are not recomputed again for each new model, unless the algorithm fails to improve the fitting. Then, only when this happens and the new model yields a worse fitting to the reference profiles, the RFs are recomputed again. In practical problems, we found that most of the time it is enough to compute brute force RFs only once and only the response to temperature (for the other parameters

we have taken the FDC response without any problems), in order to match the reference profile below the noise level of our tests.

Using this strategy we recovered the model shown in Figure 5. The fitting to the reference profiles is shown in Figure 6. Note that the recovered model is very close to VAL-C (within the error bars, in any case) and that the line profiles are matched below the noise level of the reference profiles. Therefore, the inversion code has succeeded in retrieving all the information contained in the lines.

The same test is carried out with the HOLMUL model (extrapolated to higher layers until the line transitions become optically thin) as our reference atmosphere, to verify that the code behaves equally well in the presence of cool chromospheres. Using the same combination of Ca II and Fe I lines described above, we recovered the model depicted in Figure 7 whose synthetic profile accurately matches the reference lines, as can be seen in Figure 8.

For the following example, we have synthesized a reference set of lines trying to match the specifications expected for typical observations of the Advanced Stokes Polarimeter (ASP; see Elmore et al. 1992), managed by the High Altitude Observatory. To this aim, we have selected the two lines of Fe I at 6301 Å and 6302 Å (again, treated under LTE), and the Mg I lines b_1 and b_2 at 5183 Å and 5173 Å, respectively, and computed the synthetic profiles emergent from the VAL-C model, sampling the lines with a spectral resolution of 20 mÅ. For the NLTE lines we employed a Mg I–Mg II model atom considering 12 levels plus continuum (see Uitenbroek 1997). The results are summarized in Figure 9. The inversion now succeeds in recovering a model that accurately matches all the four reference lines (see Fig. 10). Only the photosphere is accurately recovered, and very little information can be obtained regarding the temperature minimum region. However, we stress that in this test the reference profiles are accurately reproduced. Therefore the lack of information on the temperature minimum and the chromospheric layers is solely due to the fact that for this model the set of spectral lines chosen do not carry out that information. It is also important to note that for this inversion it was not necessary to use the brute force approach for the RFs because the FDC approximation was accurate enough to match the reference profiles below the noise level. This result could have been expected from our discussion in the preceding section when it was shown that the FDC RFs were very accurate for these lines and model (see Fig. 2).

From the results of this last test, we might be tempted to conclude that these Mg I lines are not very useful for the study of the solar chromosphere. However, this is not necessarily the case since the picture significantly changes when a different reference atmosphere is considered. We now choose the MACKKL sunspot model as our reference atmosphere, modified to include a macroscopic line-of-sight velocity that increases with height.

This problem is particularly interesting due to the fact that there is a very steep change in temperature near $\log(\tau_{500}) = -5$, thus introducing a further complication in the inversion since, as stated above, the code assumes that the corrections on the current model estimation are smooth in between the nodes. The reference spectrum was given as input to the inversion code. In Figure 11 we immediately see that there is an obvious difficulty in reproducing the temperature discontinuity with our smooth model (derived

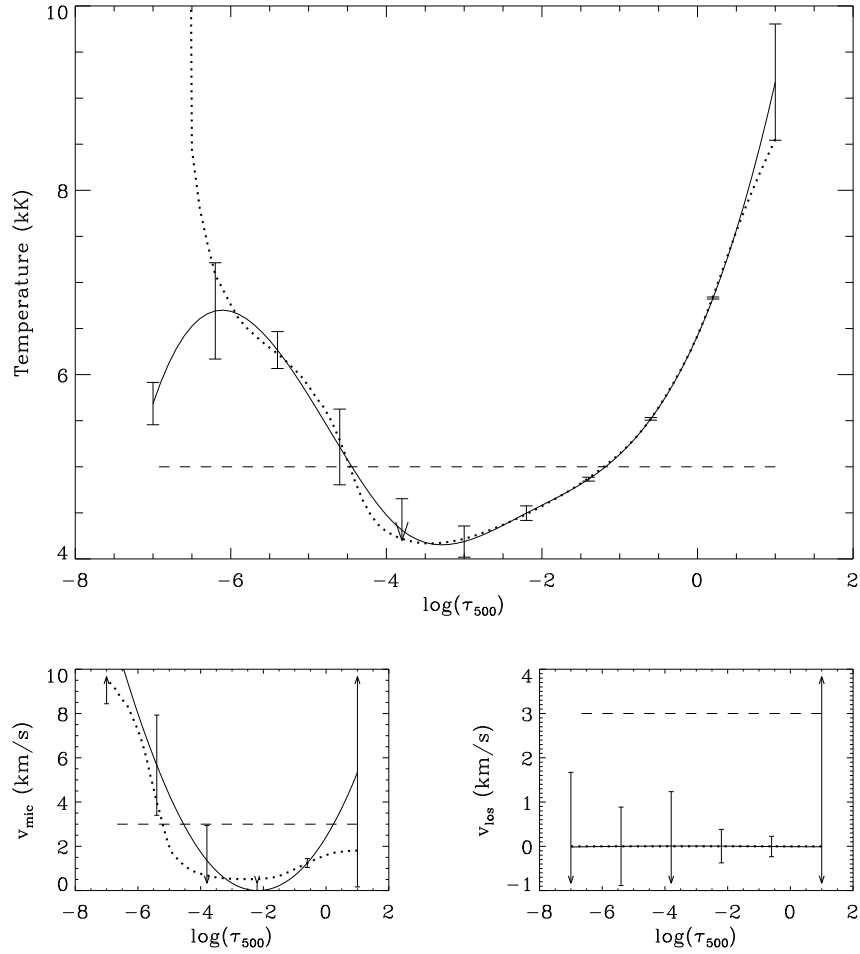


FIG. 3.—FDC inversion of four NLTE Ca II lines and a photospheric LTE Fe I line. *Dotted line*: Reference model (VAL-C). *Solid line*: Recovered model. *Dashed line*: Starting guess. An arrow at the end of an error bar indicates that this bar extends outside the range of the plot. Reference macroturbulence: 2.00 km s^{-1} . Recovered: $1.96 \pm 0.26 \text{ km s}^{-1}$. Starting guess: 0.50 km s^{-1} .

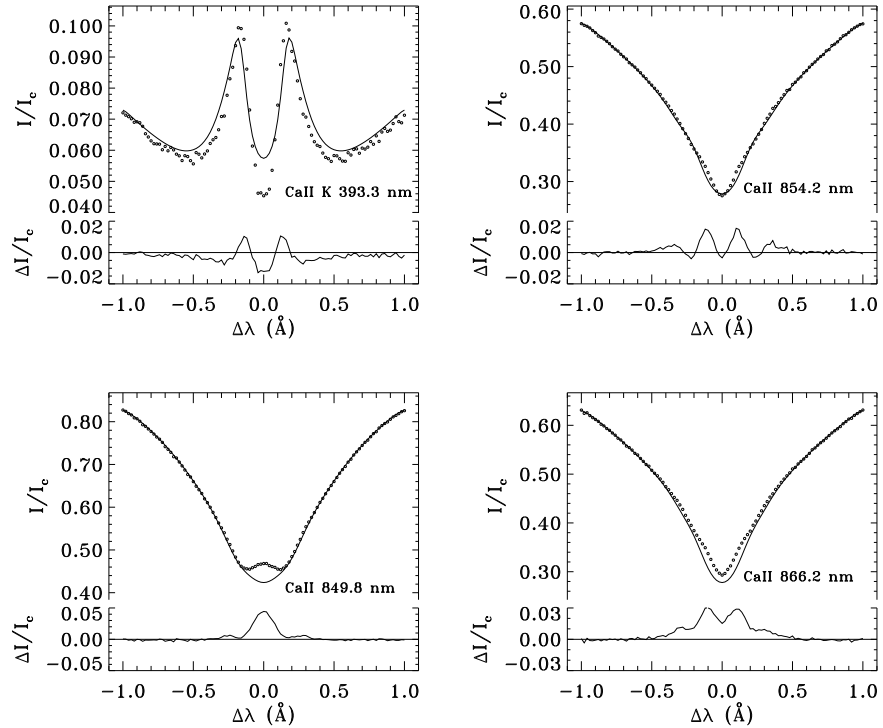


FIG. 4.—Synthetic and reference profiles (see Fig. 3). *Dotted line*: Reference profiles. *Solid line*: Synthetic profiles. Residuals are shown below each panel.

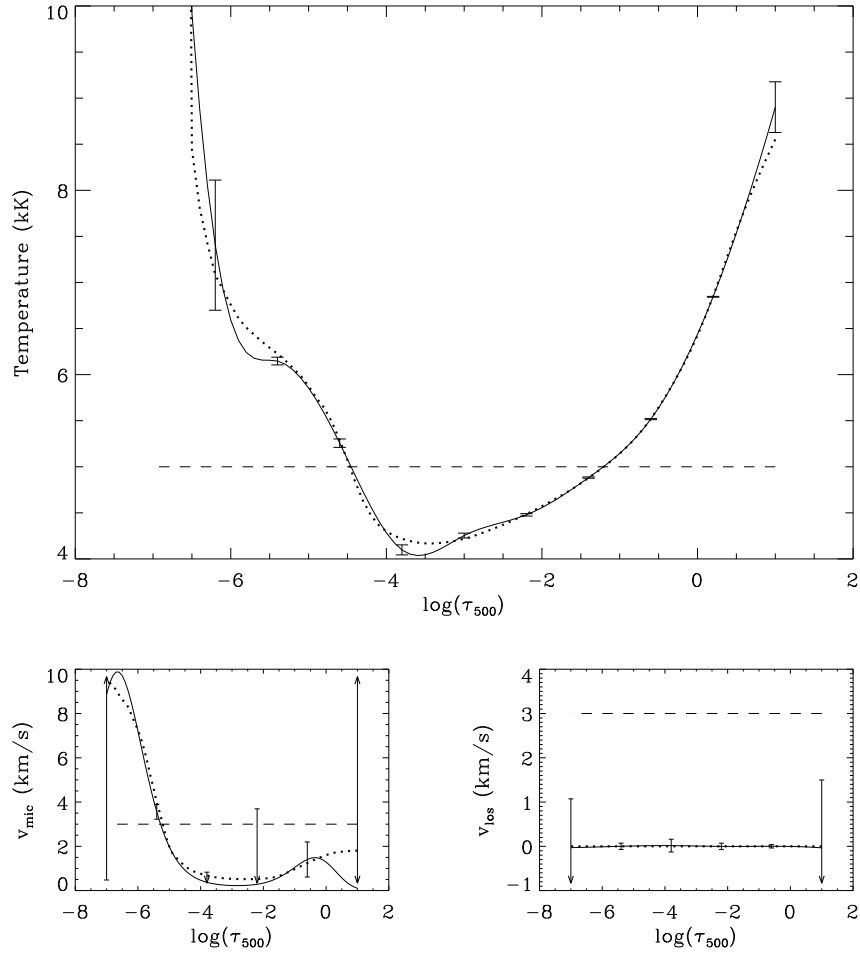


FIG. 5.—Inversion of four NLTE Ca II lines and a photospheric LTE Fe I line. *Dotted line*: Reference model (VAL-C). *Solid line*: Recovered model. *Dashed line*: Starting guess. Reference macroturbulence: 2.00 km s^{-1} . Recovered: $1.98 \pm 0.16 \text{ km s}^{-1}$. Starting guess: 0.50 km s^{-1} .

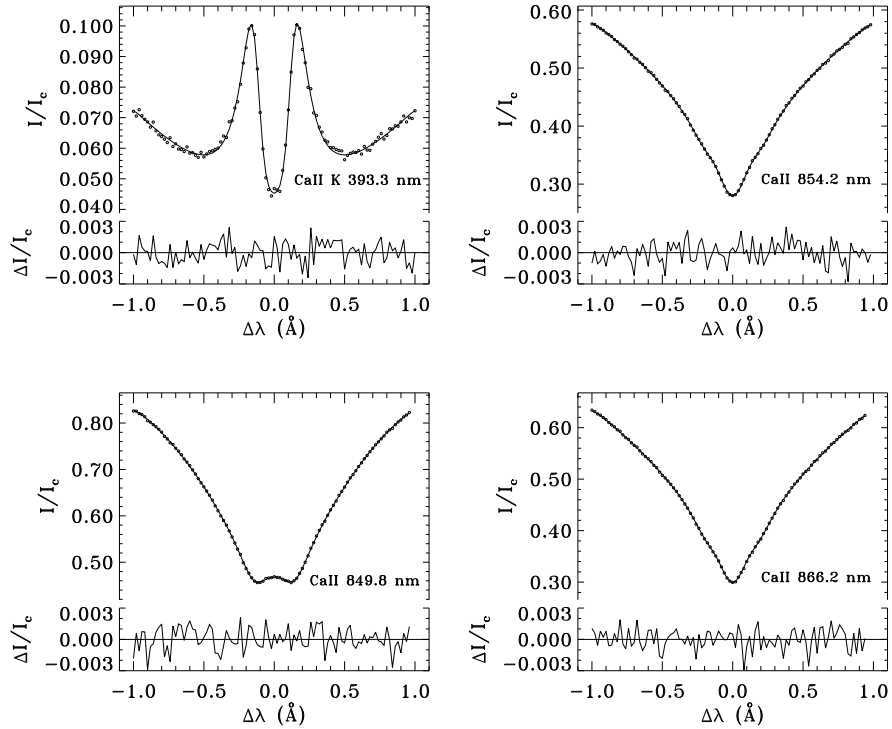


FIG. 6.—Synthetic and reference profiles (see Fig. 5). *Dotted line*: Reference profiles. *Solid line*: Synthetic profiles. Residuals are shown below each panel.

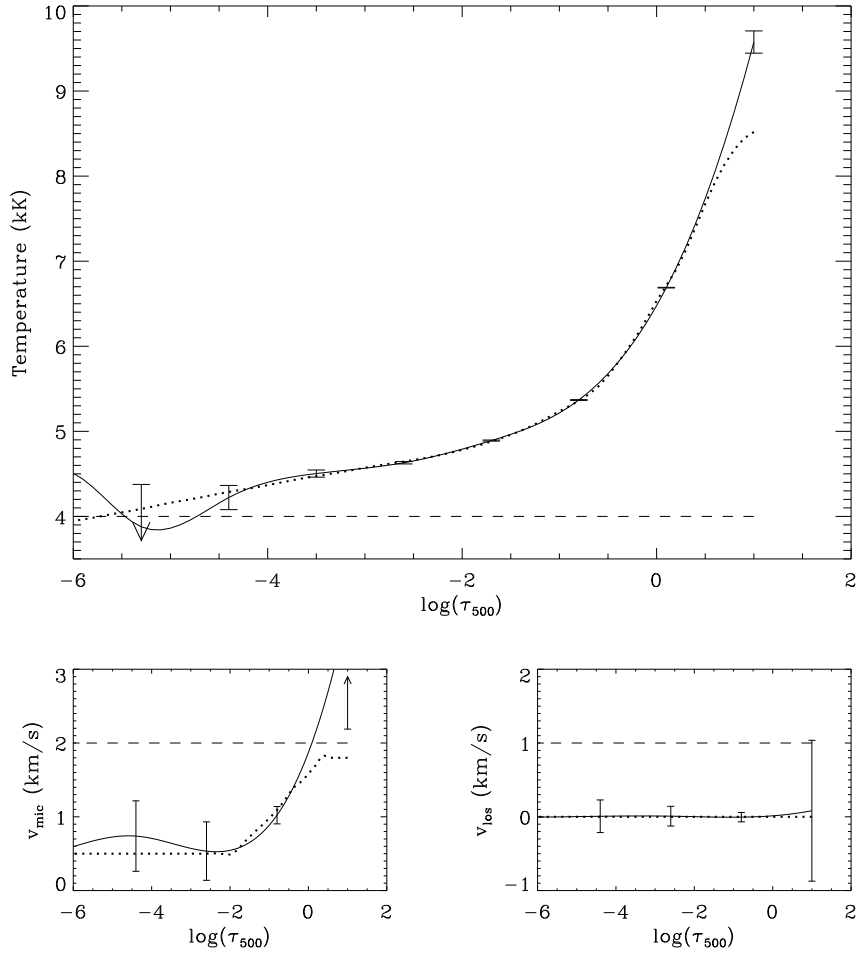


FIG. 7.—Inversion of four NLTE Ca II lines and a photospheric LTE Fe I line. *Dotted line*: Reference model (HOLMUL). *Solid line*: Recovered model. *Dashed line*: Starting guess. Reference macroturbulence: 1.60 km s^{-1} . Recovered: $1.56 \pm 0.16 \text{ km s}^{-1}$. Starting guess: 0.50 km s^{-1} .

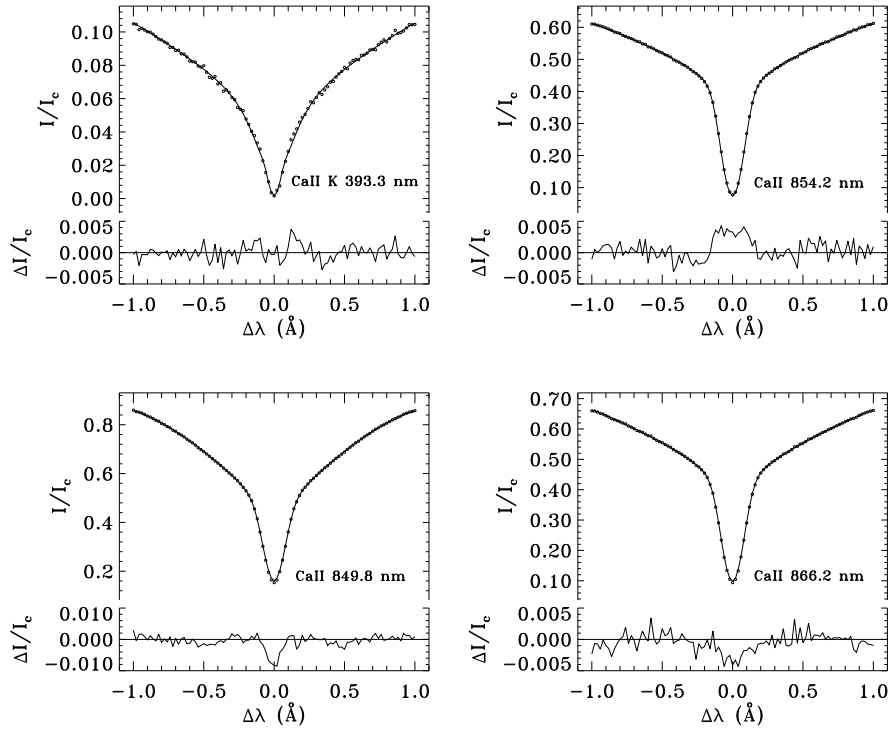


FIG. 8.—Synthetic and reference profiles (see Fig. 7). *Dotted line*: Reference profiles. *Solid line*: Synthetic profiles. Residuals are shown below each panel.

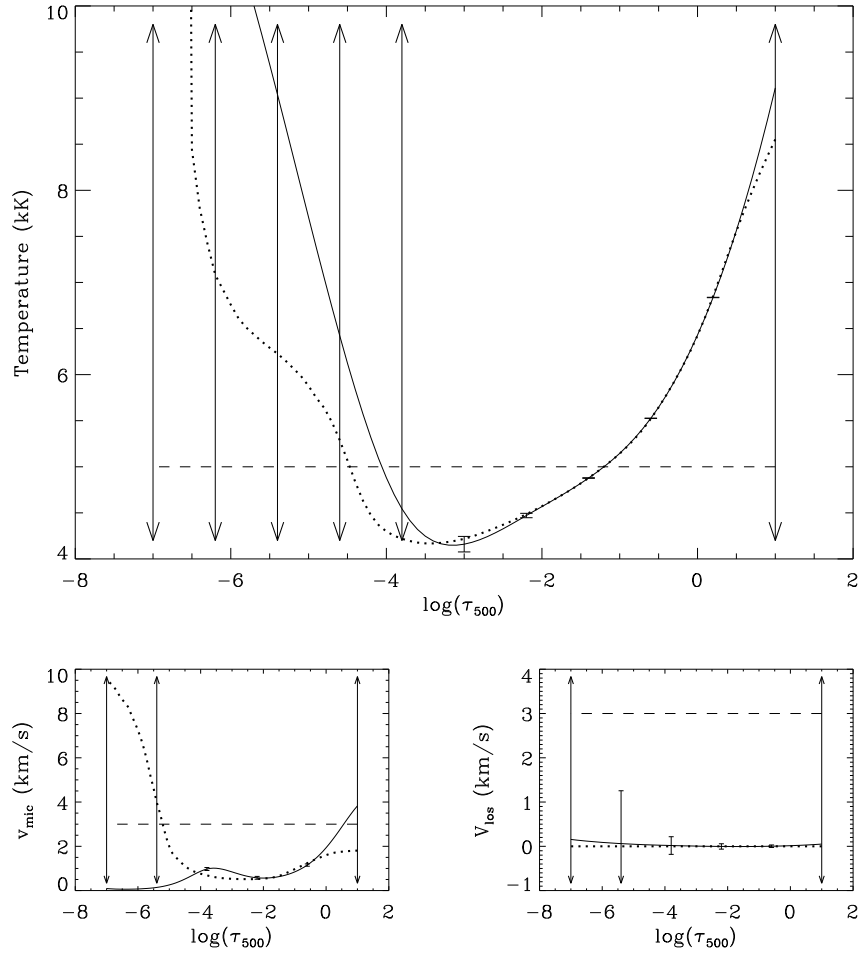


FIG. 9.—Inversion of the LTE Fe I lines at 630.1 and 630.2 nm and the NLTE Mg I b_1 and b_2 lines. *Dotted line*: Reference model (VAL-C). *Solid line*: Recovered model. *Dashed line*: Starting guess. Reference macroturbulence: 1.50 km s^{-1} . Recovered: $1.50 \pm 0.01 \text{ km s}^{-1}$. Starting guess: 0.50 km s^{-1} .

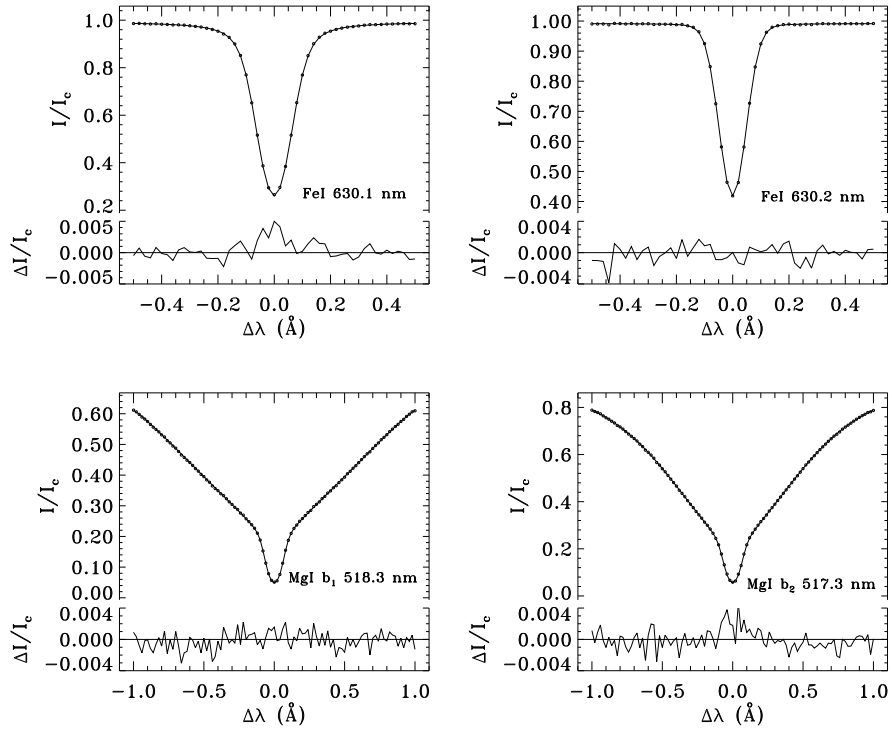


FIG. 10.—Synthetic and reference profiles (see Fig. 9). *Dotted line*: Reference profiles. *Solid line*: Synthetic profiles. Residuals are shown below each panel.

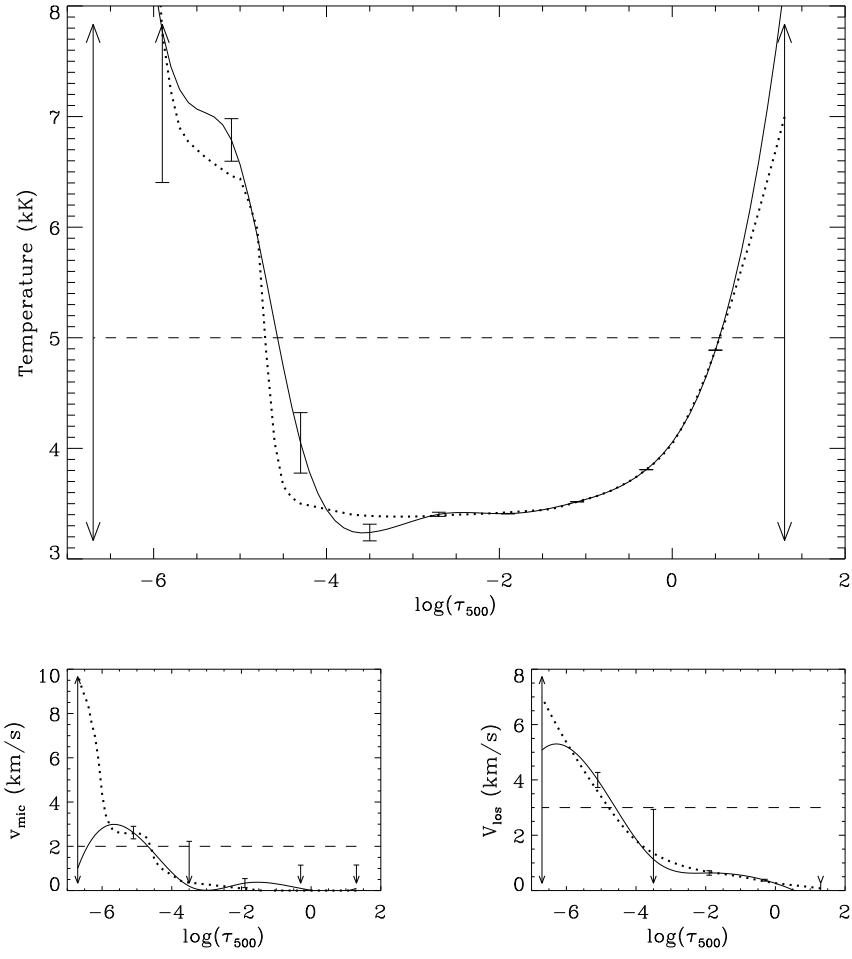


FIG. 11.—Inversion of the LTE Fe I lines at 630.1 and 630.2 nm and the NLTE Mg I b_1 and b_2 lines. *Dotted line*: Reference model (Maltby et al. 1986). *Solid line*: Recovered model. *Dashed line*: Starting guess. Reference macroturbulence: 3.00 km s^{-1} . Recovered: $3.01 \pm 0.12 \text{ km s}^{-1}$. Starting guess: 0.50 km s^{-1} .

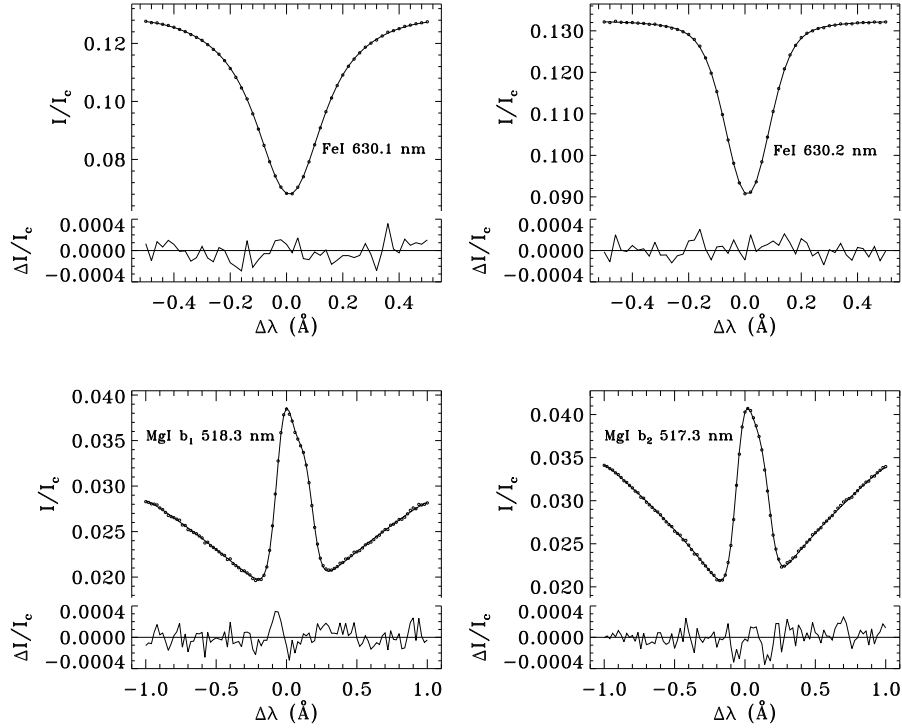


FIG. 12.—Synthetic and reference profiles (see Fig. 11). *Dotted line*: Reference profiles. *Solid line*: Synthetic profiles. Residuals are shown below each panel.

from a cubic splines interpolation of the model parameters at the inversion nodes). The set of lines chosen is most sensitive around $\log(\tau_{500}) = -5$ (see Fig. 2), so that the inversion is able to recover this region. However, around $\log(\tau_{500}) = -4$, where the sensitivity is much smaller, we obtain a model that is hotter above $\log(\tau_{500}) = -4$ and cooler below that point. Figure 12 shows that there is a good agreement between the synthetic and observed profiles because the effects of these hotter and cooler layers on the emergent profile cancel out and we end up with a synthetic spectrum that is very similar to that produced by the MACKKL model. Note also that the microturbulence and the velocity field are well recovered up to $\log(\tau_{500}) = -6$.

6. CONCLUSIONS

We have developed and tested an NLTE inversion code of spectral lines for the recovery of the atmospheric thermodynamics, based on RFs combined with efficient NLTE methods, using the assumptions of one-dimensional plane-parallel geometry and complete angle and frequency redistribution (CRD). This code provides a new valuable diagnostic tool for the understanding of the thermal and dynamical processes that occur in the solar and stellar chromospheres.

A combination of approximate analytical with strict numerical RFs brings the whole procedure into affordable CPU requirements so that practical applications can be properly tackled with this technique. Numerical tests show the reliability of our method, as well as the validity of the computed error bars to set the confidence limits of the recovered models.

We believe that there are two important aspects for the future development of this technique. The generalization of the code to deal with the full Stokes vector would open a wide field of applications related to the analysis of the polarization state of strong lines. Valuable information could then be obtained regarding the magnetic structure of the atmosphere. Another important point is the inclusion of partial redistribution effects, making the code suitable for the inversion of very strong lines that carry out precious information on the physical conditions in the higher chromosphere. We are currently working on these two generalizations.

Computational advantages can be obtained with some extra effort on the optimization of the code. Dramatic improvements in CPU time would be obtained with the inclusion of the Gauss-Seidel or successive overrelaxation (SOR) iterative method developed by Trujillo Bueno & Fabiani Bendicho (1995) for the solution of the NLTE radiative transfer problems. Also, a better approximation for the RFs could be useful to save a significant amount of CPU time that is spent in their numerical calculation.

Finally, and most important, the application of this new diagnostic tool to the analysis of real observations may improve our current understanding of the solar and stellar chromospheres.

We are grateful to N. G. Shchukina for kindly providing us with her background opacity package and to H. Uitenbroek for supplying some atomic models that we have used in our computations. Partial support by the Spanish Dirección General de Educación Superior through project PB 95-0028 is gratefully acknowledged.

REFERENCES

- Allende Prieto, C., Ruiz Cobo, B., & García López, R. 1998, *ApJ*, 502, 951
 Beckers, J. M., & Milkey, R. W. 1975, *Sol. Phys.*, 43, 289
 Bellot Rubio, L. R., Ruiz Cobo, B., & Collados, M. 1997, *ApJ*, 478, L45
 Caccin, R., Gómez, M. T., Marmolino, C., & Severino, G. 1977, *A&A*, 54, 227
 Collados, M., Martínez Pillet, V., Ruiz Cobo, B., del Toro Iniesta, J. C., & Vázquez, M. 1994, *A&A*, 291, 622
 del Toro Iniesta, J. C., Tarbell, T. D., & Ruiz Cobo, B. 1994, *ApJ*, 436, 400
 Elmore, D. F., et al. 1992, *Proc. SPIE*, 1746, 22
 Fabiani Bendicho, P., Trujillo Bueno, J., & Auer, L. H. 1997, *A&A*, 324, 161
 Holweger, H., & Müller, E. A. 1974, *Sol. Phys.*, 39, 19 (HOLMUL)
 Kalkofen, W. 1987, *Numerical Radiative Transfer*, ed. W. Kalkofen (Cambridge: Cambridge Univ. Press)
 Kostik, R. I., Shchukina, N. G., & Rutten, R. J. 1996, *A&A*, 305, 325
 Maltby, P., Avrett, E. H., Carlsson, M., Kjeldseth-Moe, O., Kurucz, R. L., & Loeser, R. 1986, *ApJ*, 306, 284 (MACKKL)
 Marquardt, D. W. 1963, *SIAM J. Appl. Math.*, 11, 431
 Mein, P. 1971, *Sol. Phys.*, 20, 3
 Mein, P., Mein, N., Malherbe, J. M., & Dame, L. 1987, *A&A*, 177, 283
 Mihalas, D. 1978, *Stellar Atmospheres* (New York: Freeman)
 Press, W. H., Flannery, B. P., Teukolsky, S. A., & Vetterling, W. T. 1986, *Numerical Recipes* (Cambridge: Cambridge Univ. Press)
 Rodríguez Hidalgo, I., Ruiz Cobo, B., & Collados, M. 1996, in *ASP Conf. Ser. 109, Cool Stars, Stellar Systems, and the Sun*, ed. R. Pallavicini & A. K. Dupree (San Francisco: ASP), 151
 Ruiz Cobo, B., & del Toro Iniesta, J. C. 1992, *ApJ*, 398, 375
 Ruiz Cobo, B., del Toro Iniesta, J. C., Rodríguez Hidalgo, I., Collados, M., & Sánchez Almeida, J. 1995, *Joint Organization for Solar Observations Annual Report*, 162
 ———. 1996, in *ASP Conf. Ser. 109, Cool Stars, Stellar Systems, and the Sun*, ed. R. Pallavicini & A. K. Dupree (San Francisco: ASP), 155
 Ruiz Cobo, B., Rodríguez Hidalgo, I., & Collados, M. 1997, *ApJ*, 488, 462
 Rybicki, G. B., & Hummer, D. G. 1991, *A&A*, 245, 171
 ———. 1992, *A&A*, 262, 209
 Sánchez Almeida, J. 1997, *ApJ*, 491, 993
 Shchukina, N. G., & Trujillo Bueno, J. 1997, in *ASP Conf. Ser. 118, First Advances in Solar Physics Euroconference: Advances in the Physics of Sunspots*, ed. B. Schmieder, J. C. del Toro Iniesta, & M. Vázquez (San Francisco: ASP), 207
 Shchukina, N. G., Trujillo Bueno, J., & Kostik, R. I. 1997, *Sol. Phys.*, 172, 117
 Socas-Navarro, H., & Trujillo Bueno, J. 1997, *ApJ*, 490, 383
 Socas-Navarro, H., Trujillo Bueno, J., Ruiz Cobo, B., & Shchukina, N. G. 1996, *Joint Organization for Solar Observations Annual Report*, 86
 Teplitskaya, R. B., Grigoryeva, S. A., & Skochilov, V. G. 1996, *A&AS*, 115, 209
 Teplitskaya, R. B., Skochilov, V. G., & Grigoryeva, S. A. 1992, *Kinematika i fizika nebes. tel* 8, 1, 3
 Teplitskaya, R. B., Turova, I. P., & Skochilov, V. G. 1992, *Kinematika i fizika nebes. tel* 8, 3, 27
 Trujillo Bueno, J., & Fabiani Bendicho, P. 1995, *ApJ*, 455, 646
 Uitenbroek, H. 1989, *A&A*, 213, 360
 ———. 1997, *Solar Phys.*, 172, 109
 Vernazza, J. E., Avrett, E. H., & Loeser, R. 1981, *ApJS*, 45, 635 (VAL-C)
 Westendorp Plaza, C., del Toro Iniesta, J. C., Ruiz Cobo, B., Martínez Pillet, V., Lites, B. W., & Skumanich, A. 1997a, in *ASP Conf. Ser. 118, First Advances in Solar Physics Euroconference: Advances in the Physics of Sunspots*, ed. B. Schmieder, J. C. del Toro Iniesta, & M. Vázquez (San Francisco: ASP), 202
 ———. 1997b, *Nature*, 389, 47